PHYSICAL REVIEW D **81,** 015011 (2010)

Littlest Higgs model with T parity and top quark pair production at LHC

Jin-Yan Liu,[1] Zong-Guo Si,[2] and Chong-Xing Yue[1]
[1]*Department of Physics, Liaoning Normal University, Dalian 116029, P. R. China*
[2]*School of Physics, Shandong University, Jinan Shandong 250100, P. R. China*[*]
(Received 7 September 2009; published 21 January 2010)

We consider the top-quark pair production at the upcoming LHC and investigate the contributions of the new particles to the related observables within the framework of the littlest Higgs model with T-parity(LHT). It is found that the LHT model can generate significant corrections to the $t\bar{t}$ production cross section and their spin correlations.

DOI: 10.1103/PhysRevD.81.015011 PACS numbers: 12.60.Cn, 12.15.Lk, 13.38.Dg

I. INTRODUCTION

The top quark, first observed at Fermilab in 1995 [1,2], is the heaviest fundamental fermion discovered to date. It may play an important role in the mechanism of electroweak symmetry breaking (EWSB) [3], and especially new physics connected to EWSB may be found through precision studies of top-quark observables. Compared with lighter quarks, which are permanently confined in bound states with other quarks or antiquarks, the lifetime of the top quark is extremely short so that its properties are not polluted by the hadronization process. Due to the $V-A$ interaction within the standard model (SM), top-quark spin information can be transferred into its decay products [4]. In particular, phenomena associated with their spins are reflected directly in the distributions and the corresponding angular correlations of their decay products, eg., jet, w-boson, or charged lepton. These distributions are determined by the t and $\bar{t}$ polarizations and spin correlations induced by the production mechanism(s). Hence spin-polarization and spin-correlation phenomena can provide valuable information about the interactions of top quarks. An attempt to detect these spin correlations in a small $t\bar{t}$ dilepton sample collected at the Tevatron was recently reported by the D0 collaboration [5]. Furthermore, it is possible to measure the observables that depend on the top-quark spin, providing a good probe for tests of the SM and for searches for new physics beyond the SM.

At LHC, huge number events of top quarks will be produced every year. It is possible to measure the top-quark properties with high precision at this facility in order to search for new physics beyond the SM. As far as theoretical predictions on top-quark pair production are concerned, the cross sections for spin-averaged top-quark pair production have been known at next-to-leading order (NLO) in QCD [6–8]. As to top-quark spin phenomena at hadron colliders there exists an extensive literature on theoretical investigations within the SM [9–15] and beyond [16–23], There are also several studies of effects of new physics models on the top spin correlations [24–26].

For the existence of the large enhancement to the Yukawa coupling in new physics models, studying the Yukawa electroweak radiative corrections is specially interesting. By far, a lot of works have appeared to study the non-SM one-loop corrections to the top-quark pair production at LHC in the context of new physics models, such as minimal supersymmetric standard model [27–29] and two-Higgs-doublet model [30]. In this paper, we focus on studying the hadronic top-quark pair production and decay at leading order LO under the framework of the littlest Higgs model with T-parity(LHT) [31–34] by taking the spin information of the top quarks into account.

The layout of the present paper is as follows: the essential features of the LHT model [31–34] related to our work is briefly reviewed in Sec. II. The radiative corrections to the top-quark pair production at LHC is investigated, and the related numerical results for the total cross section, the spin asymmetry, etc. are obtained in Sec. III. Finally the conclusion and a short discussion are given.

II. THE ESSENTIAL FEATURES OF THE LHT MODEL

The LHT model is based on a $SU(5)/SO(5)$ global symmetry breaking pattern. A subgroup $[SU(2)\times U(1)]_1\times[SU(2)\times U(1)]_2$ of the $SU(5)$ global symmetry is gauged and at the scale f it is broken into the SM electroweak symmetry $SU(2)_L\times SU(1)_Y$. Under T-parity, particle fields are divided into T-even and T-odd sectors. The T-even sector consists of the SM particles and a heavy top-quark T_+, while the T-odd sector contains heavy gauge bosons (B_H, Z_H, $W_H^{\pm}$), a scalar triplet (Φ), and a copy of leptons and quarks.

We use the Goldstone-boson equivalence theorem (ET) [35–39] to calculate the leading electroweak Yukawa contributions to the anomalous $gt\bar{t}$ coupling, and adopt the notations as: h is the Higgs boson; π^0, $\pi^{\pm}$ is eaten by SM gauge bosons Z and W; η, ω^0, $\omega^{\pm}$ are eaten by the T-odd heavy gauge bosons B_H, Z_H, $W_H^{\pm}$, respectively. In T-odd sector, there are three heavy quarks t_-, b_-, and T_- contributing to $gt\bar{t}$ coupling, which are T-parity partners of SM top, bottom quarks and the heavy T-even T_+ quark.

[*]jinyan_liu1987@163.com

At the order of v^2/f^2, the masses of the T-odd set of the $SU(2) \times U(1)$ gauge bosons are given by:

$$M_{B_H} = \frac{g' f}{\sqrt{5}}\left[1 - \frac{5v^2}{8f^2}\right],$$
$$M_{Z_H} \approx M_{W_H} = gf\left[1 - \frac{v^2}{8f^2}\right]. \quad (1)$$

Where $v = 246$ GeV is the scale of the EWSB, g' and g are the SM $U(1)_Y$ and $SU(2)_L$ gauge coupling constants, respectively. Because of the smallness of g', the gauge boson B_H is the lightest T-odd particle, which is stable, electrically neutral, and weakly interacting particle. Thus, it can be seen as an attractive dark matter candidate [34].

Assuming there is flavor universal and diagonal Yukawa coupling k, the T-odd quarks for different family will be degenerate in mass, and the masses of the up- and down-type T-odd fermions can be written as:

$$M_{t_-} \approx \sqrt{2}kf\left(1 - \frac{v^2}{8f^2}\right), \qquad M_{b_-} \approx \sqrt{2}kf. \quad (2)$$

Being $f \geq 500$ GeV, it is clear from Eq. (2) that there is $M_{t_-} \approx M_{b_-}$.

As for the heavy T-even T_+ quark and its partner T_-, their masses are given by [40]:

$$M_{T_+} = \frac{f}{v}\frac{m_t}{\sqrt{X_L(1-X_L)}}\left[1 + \frac{v^2}{f^2}\left(\frac{1}{3} - X_L(1-X_L)\right)\right], \quad (3)$$

$$M_{T_-} = \frac{f}{v}\frac{m_t}{\sqrt{X_L}}\left[1 + \frac{v^2}{f^2}\left(\frac{1}{3} - \frac{1}{2}X_L(1-X_L)\right)\right], \quad (4)$$

where $X_L = \lambda_1^2/(\lambda_1^2 + \lambda_2^2)$ is the mixing parameter between the SM top-quark t and the new top-quark T_+, in which λ_1 and λ_2 are the Yukawa coupling parameters.

In this paper we use the 't Hooft-Feyman gauge, so the Goldstone-Boson mass is the same as its corresponding gauge boson, that is to say:

$$m_{\omega^{\pm,0}} = M_{W_H}, \qquad m_\eta = M_{B_H}. \quad (5)$$

III. TOP-QUARK PAIR PRODUCTION AND DECAYS OF THE POLARIZED TOP QUARK AT LHC

At hadron colliders, top-quark pair $t\bar{t}$ is produced predominantly by the strong interactions. At the LHC, their production is mainly due to gluon gluon fusion, while $q\bar{q}$ annihilation contribute only a small part. In the context of the LHT model, the Feynman diagrams for the processes contributing to $t\bar{t}$ pair production are depicted in Fig. 1. Note that the black dot in Fig. 1. represents the effective $gt\bar{t}$ vertex induced by the new particles predicted in the LHT model. The effective $gt\bar{t}$ vertex receives the contributions from the interactions like $(h - t - T_+)$, $(\pi^0 - t - T_+)$, $(\omega^0 - t - t_-)$, $(\eta - t - t_-)$, $(\omega^- - t - b^-)$, and $(\eta - t - T_-)$. The corresponding Feynman rules can be found in [40]. Note that the interaction between the scalar triplet Φ and top quark also exists, but its contribution is small and can be neglected.

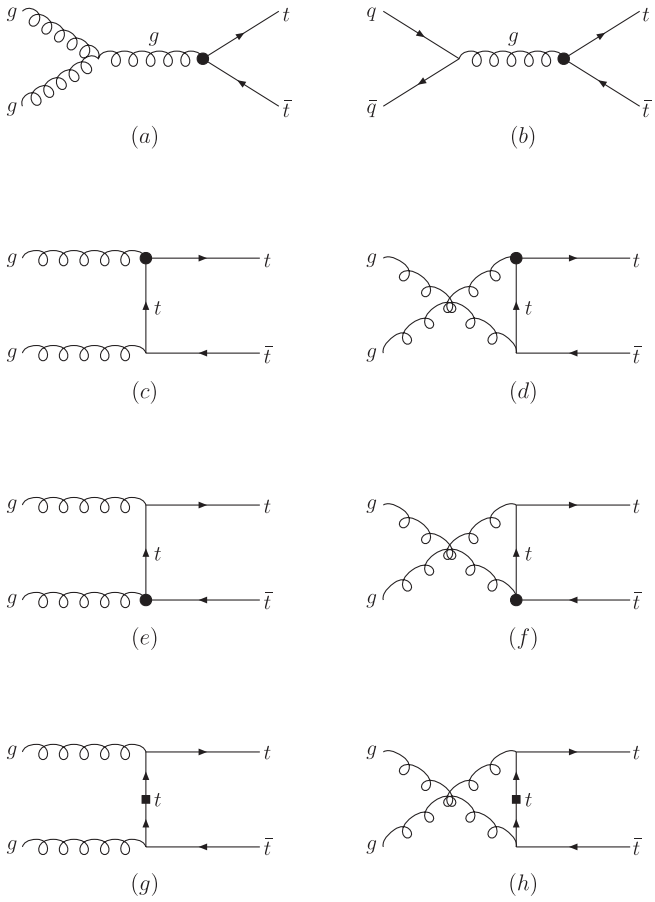

FIG. 1. Feynman diagrams for $t\bar{t}$ pair production contributed from LHT.

The invariant amplitudes for the processes $g(p_1) \times g(p_2) \to t(k_1, s_t)\bar{t}(k_2, s_{\bar{t}})$ and $q(p_1')\bar{q}(p_2') \to t(k_1, s_t)\bar{t}(k_2, s_{\bar{t}})$ can be written as follows:

$$M_a = g_s^2 T^a f^{abc}(p_1 - p_2)_\sigma \epsilon^\mu(p_1)\epsilon^\nu(p_2)\frac{g_{\mu\nu}}{(p_1+p_2)^2} \times \bar{u}(k_1, s_t)[A_a\gamma^\sigma + iB_a\sigma^{\sigma\alpha}(p_1+p_2)_\alpha + C_a\left(\gamma^\sigma - \frac{2m_t}{(p_1+p_2)^2}(p_1+p_2)^\sigma\right)]\nu(k_2, s_{\bar{t}}); \quad (6)$$

$$M_b = -ig_s^2 T^a T^b \bar{v}(p_1')\gamma^\mu u(p_2')\frac{g_{\mu\nu}}{(p_1'+p_2')^2}\bar{u}(k_1, s_t) \times \left[A_a\gamma^\nu + iB_a\sigma^{\nu\alpha}(p_1'+p_2')_\alpha + C_a\left(\gamma^\sigma - \frac{2m_t}{(p_1'+p_2')}(p_1'+p_2')^\sigma\right)\right]\nu(k_2, s_{\bar{t}}); \quad (7)$$

$$M_c = -ig_s^2 T^a T^b \epsilon^\mu(p_1)\epsilon^\nu(p_2)\bar{u}(k_1, s_t) \times [A_c\gamma_\mu + B_c(k_1 - p_1)_\mu \not{p}_1 + C_c(k_1 - p_1)_\mu \gamma^5 + D_c(k_1 - p_1)_\mu \not{p}_1\gamma^5 + E_c(k_1 - p_1)_\mu + F_c\gamma_\mu\gamma^5 + G_c\not{p}_1\gamma_\mu + H_c\not{p}_1\gamma_\mu\gamma^5]\frac{(\not{k}_1 - \not{p}_1 + m_t)}{(k_1 - p_1)^2 - m_t^2} \times \gamma_\nu\nu(k_2, s_{\bar{t}}); \quad (8)$$

$$M_e = -ig_s^2 T^a T^b \epsilon^\mu(p_1)\epsilon^\nu(p_2)\bar{u}(k_1, s_t)\gamma_\mu \frac{(\not{k}_1 - \not{p}_1 + m_t)}{(k_1 - p_1)^2 - m_t^2} \times [A_e\gamma_\nu + B_e(k_1 - p_1)_\nu \not{p}_2 + C_e(k_1 - p_1)_\nu\gamma^5 + D_e(k_1 - p_1)_\nu \not{p}_2\gamma^5 + E_e(k_1 - p_1)_\nu + F_e\gamma_\nu\gamma^5 + G_e\not{p}_2\gamma_\mu + H_e\not{p}_2\gamma_\mu\gamma^5]\nu(k_2, s_{\bar{t}}); \quad (9)$$

$$M_g = g_s^2 T^a T^b \epsilon^\mu(p_1)\epsilon^\nu(p_2)\bar{u}(k_1, s_t)\gamma_\mu \frac{\not{k}_1 - \not{p}_1 + m_t}{(k_1 - p_1)^2 - m_t^2} \times [\tilde{\Sigma}(\not{k}_1 - \not{p}_1) + (\not{k}_1 - \not{p}_1)(\delta Z_V - \delta Z_A\gamma_5) + m_t\delta m_t]\frac{\not{k}_1 - \not{p}_1 + m_t}{(k_1 - p_1)^2 - m_t^2}\gamma_\nu\nu(k_2, s_{\bar{t}}). \quad (10)$$

Where g_s is the strong coupling strength, T is the color generator, and f^{abc} is the structure constant of $SU_c(3)$. The invariant amplitudes M_d, M_f, M_h can be, respectively, obtained from M_c, M_e, M_g under the interchange $p_1 \leftrightarrow p_2$. The form factors appearing in M_a and M_b can be found in [41], and the others are listed in the Appendix A 1 and A 2. We also list the counterterms δZ_V, δZ_A etc. in Appendix A 3.

For the process

$$pp/(p\bar{p}) \to t\bar{t}, \quad (11)$$

the corresponding differential cross section can be written as follows

$$\frac{d\sigma_{\rm tot}}{dX} = \sum_{ab}\int dx_1 dx_2 f_{a/p}(x_1, \mu_F) f_{b/p}(x_2, \mu_F)\frac{d\hat{\sigma}(\hat{s})}{dX}, \quad (12)$$

where X can be chosen to be the $t\bar{t}$ invariant mass $M_{t\bar{t}}$ or the transverse momentum P_T of top quark, etc. $\hat{s} = x_1x_2s$ is the effective center-of-mass energy squared for the partonic process. $ab = q\bar{q}$ or gg, and $f_{a/p}(x, \mu_F)$ denotes the parton distribution function (PDF) of parton a in hadron p. In our numerical calculation, we use CTEQ6.1L [42] and set the factorization scale $\mu_F = m_t = 172.7$ GeV.

In the LHT model, the total cross section $\sigma_{\rm tot}$ which contains both the LHT and SM contributions depends on the free parameters f, k, and X_L. About the involved parameters f, some constraints come from the electroweak precision data [34], which, however, depend on the masses of T-odd fermions and the parameter δ_c (its value is related to the details of the ultraviolet completion of the theory). Hence, in our numerical calculations we relax the constraints on the parameters f, and let it vary in the range 500 GeV $\le f \le$ 2000 GeV. For X_L is the mixing parameter between the SM top-quark t and the new top-quark T_+, which exact formula has been given in Sec. II and its value in the range $0 \le X_L \le 1$. And k is a parameter at the order of 1, which varies in the range $0.11 \le k \le 4.8$ [43]. To simply our calculation, we fix $k = 0.6$ and take f and X_L as free parameters.

To illustrate the contributions of the LHT model to the production cross section σ of the process $pp \to t\bar{t}$, we define the relative ratio as follows:

$$R_1 = \left|\frac{\sigma_{\rm tot} - \sigma_{\rm SM}}{\sigma_{\rm SM}}\right|, \quad (13)$$

where $\sigma_{\rm SM}$ include only the SM contributions. The numerical results for R_1 as a function of the scale parameter f for three different X_L values with $\sqrt{s} = 10(14)$ TeV are displayed in Fig. 2(a) and 2(b). One can find that the value of R_1 increases as the parameters X_L increases and f decreases. For $X_L = 0.2$ and 500 GeV $\le f \le$ 2000 GeV, the value of R_1 is in the range of $0.2 \sim 0.15$. But for $X_L = 0.8$, its value nearly increase to 1, which means that the correction of the LHT model to the $t\bar{t}$ production cross section can reach 100%.

To see whether the observables can be measured in the upcoming LHC, in Fig. 3 we plot σ_1, σ_2 by allowing f to vary from 500 GeV to 2000 GeV and fix $X_L = 0.4$. Here we also show the required cross sections $\bar{\sigma}$ for one $t\bar{t}$ pair event produced at the LHC with the integrated luminosity of 300^{-1} fb. The cross section $\bar{\sigma}$ is defined as follows:

$$\bar{\sigma} = \frac{1 \text{ event}}{300 \text{ fb}^{-1}}. \quad (14)$$

Note that $\sigma_{1,2}$ is the results for $\sqrt{s} = 10(14)$ TeV, respectively. One can find from our results that at the LHC, the observable is under the LHC detect ability. So our results can be detected in the LHC experiments.

The relative ratio $R_2(P_T)$ for the top-quark transverse momentum distribution (P_T) of the process (11) can be defined as:

$$R_2(P_T) = \left|\frac{d\sigma_{\rm tot}/dp_T - d\sigma_{\rm SM}/dp_T}{d\sigma_{\rm SM}/dp_T}\right|. \quad (15)$$

The results for $R_2(P_T)$ at LHC with $\sqrt{s} = 14$ TeV are shown in Fig. 4. For 300 GeV $\le P_T \le$ 2000 GeV, $R_2(P_T)$ varies in the range $0.55 \sim 0.2$, $0.6 \sim 0.4$, $0.65 \sim 0.5$ for $f = 2000$ GeV, 1000 GeV and 500 GeV, respectively.

We can also define a similar observable $R_3(M_{t\bar{t}})$ related to the $t\bar{t}$ invariant mass $M_{t\bar{t}}$ distribution as follows

$$R_3(M_{t\bar{t}}) = \left|\frac{d\sigma_{\rm tot}/dM_{t\bar{t}} - d\sigma_{\rm SM}/dM_{t\bar{t}}}{d\sigma_{\rm SM}/dM_{t\bar{t}}}\right|. \quad (16)$$

We show the results for R_3 at LHC with $\sqrt{s} = 14$ TeV for

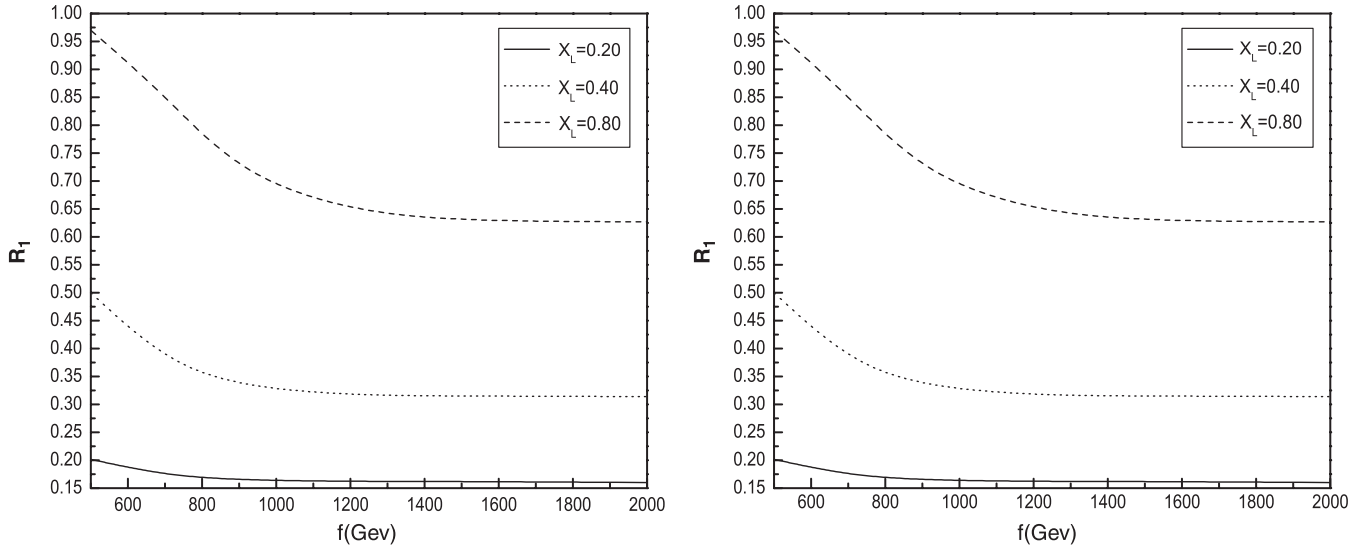

FIG. 2. R_1 as a function of the scale parameter f for three different X_L values at LHC with $\sqrt{s} = 10$ TeV(a) and $\sqrt{s} = 14$ TeV(b).

$X_L = 0.6$ and three f values in Fig. 5. One can find that R_3 drop rapidly with $m_{t\bar{t}}$ increasing. For 500 GeV $\leq m_{t\bar{t}} \leq$ 2000 GeV, R_3 is in the range of $0.29 \sim 0.23$, $0.28 \sim 0.22$ and $0.27 \sim 0.21$ for $f = 500$ GeV, 1000 GeV and 2000 GeV, respectively. Obviously the relative corrections to the top-quark transverse momentum and $t\bar{t}$ invariant mass distribution are significant and might be detected at the upcoming LHC experiments.

Finally we consider the $t\bar{t}$ spin correlations induced by LHT. We consider the process

$$pp \to t\bar{t} \to \ell^+\ell'^- + X. \tag{17}$$

The double differential distribution can be defined as [15]:

$$\frac{1}{\sigma}\frac{d\sigma^2}{d\cos\theta_{\ell^+} d\cos\theta_{\ell^-}} = \frac{1}{4}(1 + B_1\cos\theta_{\ell^+} + B_2\cos\theta_{\ell^-} - C\cos\theta_{\ell^+}\cos\theta_{\ell^-}), \tag{18}$$

where θ_{ℓ^+} (θ_{ℓ^-}) denotes the angle of the charged lepton ℓ^+ (ℓ^-) with respect to the chosen spin axis $\hat{\mathbf{a}}$ ($\hat{\mathbf{b}}$) in the top-quark (top antiquark) rest frame and σ denotes the cross section for the process (17). Here we choose the helicity basis to analyze the top spin correlation at the LHC. In this basis, the top (antitop) spin axis is regarded as the direction of motion of the top (antitop) in the top-antitop center-of-mass system. The coefficients B_1 and B_2 are associated with a polarization of the top and antitop quarks, and C reflects the strength of the $t\bar{t}$ spin correlations. In the following we focus on investigating C. Obviously, without

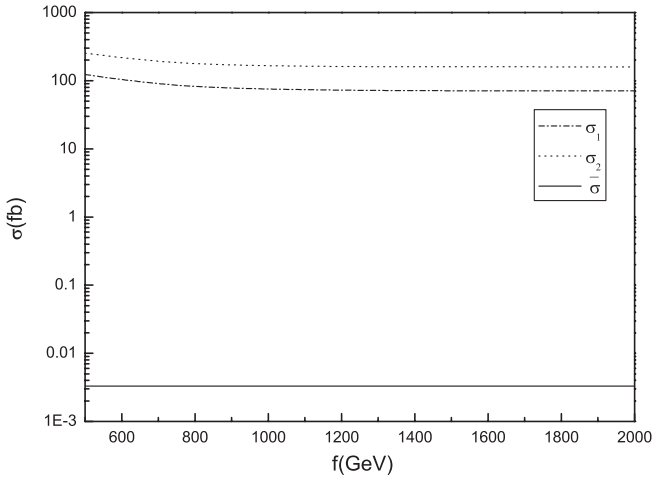

FIG. 3. The LHT model contributions to the production cross section σ as a function of the parameter f with $\sqrt{s} =$ 10(14) TeV. The horizontal solid line corresponds to the cross section $\bar{\sigma}$ for one event at the LHC with the integrated luminosity of 300^{-1} fb.

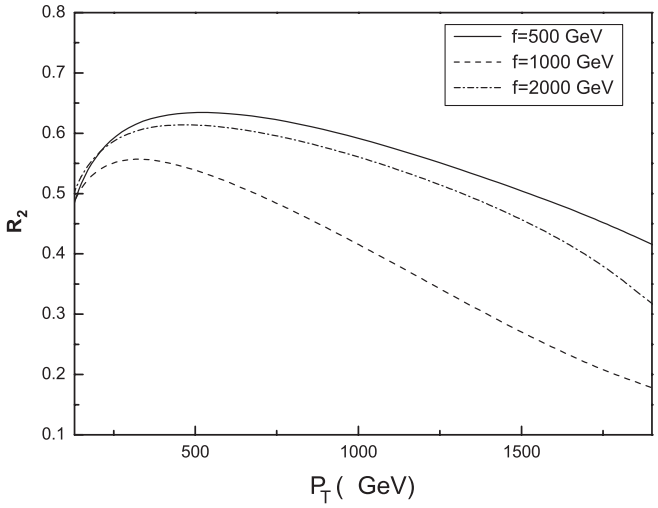

FIG. 4. R_2 as a function of the top-quark transverse momentum P_T for three values of f at the LHC with $\sqrt{s} = 14$ TeV.

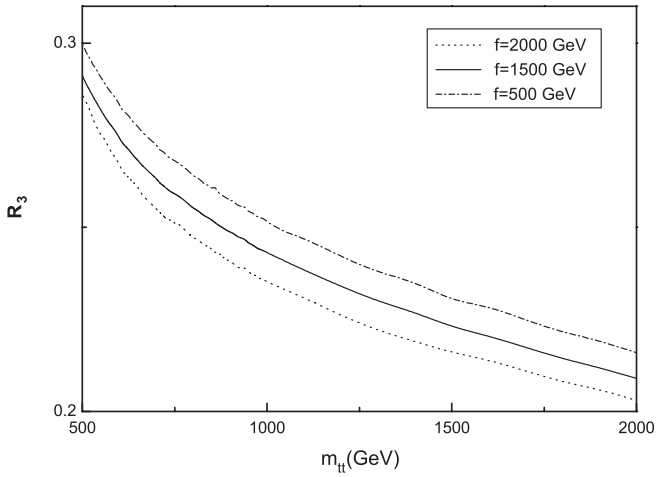

FIG. 5. The ratio R_3 as a function of $M_{t\bar{t}}$ for three values of f at LHC with $\sqrt{s} = 14$ TeV.

the acceptance cuts, C can be expressed as

$$C = 4\frac{\sigma(++) + \sigma(--) - \sigma(+-) - \sigma(-+)}{\sigma(++) + \sigma(--) + \sigma(+-) + \sigma(-+)}, \quad (19)$$

where $\sigma(+-)$ denotes the cross section for $\cos\theta_{\ell^+} > 0$ and $\cos\theta_{\ell^-} < 0$, etc. We also define a relative ratio of the $t\bar{t}$ spin correlation as follows

$$R_4 = \left| \frac{C_{\rm tot} - C_{\rm SM}}{C_{\rm SM}} \right|. \quad (20)$$

In Fig. 6 we plot the relative correction parameter R_4 as a function of the scale parameter f and three values of the mixing parameter X_L at LHC with $\sqrt{s} = 14$ TeV. One can see from Fig. 6 the ratio R_4 is sensitive to the parameter X_L and f. For 500 GeV $< f <$ ~2000 GeV, R_4 varies in the range [0.01, 0.001], [0.48, 0.05], and [1.18, 0.08] for $X_L =$ 0.4, 0.6 and 0.8, respectively. It is clear that in reasonable ranges of the free parameters, the signals induced by LHT may be detected at LHC.

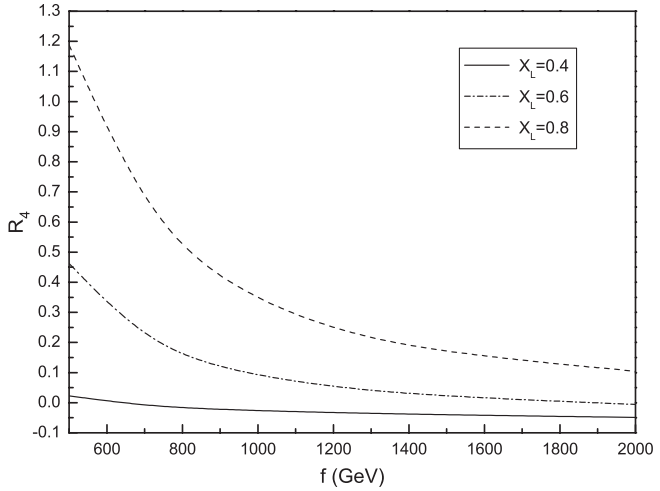

FIG. 6. The ratio R_4 as a function of f for three values of X_L at LHC with $\sqrt{S} = 14$ TeV.

IV. CONCLUSIONS AND DISCUSSIONS

The LHT model is one of the attractive little *Higgs* models. It is not only consistent with electroweak precision tests but also predicts the existence of the heavy new particles, such as new heavy top-quark (T_+, T_-), new gauge bosons (B_H, $W_H^{\pm}$, and Z_H) and T-odd fermions. These new particles might produce the observability signatures in future high energy collider experiments. In particular, these new particles can generate significant corrections to the $gt\bar{t}$ vertex and further contribute top-antitop pair production. In this paper, we investigate the relative corrections from LHT to the production cross section σ, the transverse top-momentum distribution $d\sigma/dp_T$ and the $t\bar{t}$ invariant mass distribution $d\sigma/dm_{t\bar{t}}$, etc. for the $pp \to t\bar{t}$ process at LHC. Our numerical results show that, in most of the parameter space, the LHT model can give large contributions to these observables. The possible signatures of the LHT model might be tested at the upcoming LHC.

$t\bar{t}$ spin-correlation phenomena can provide valuable information on top-quark production mechanism and its decay dynamics, and can be used as good tool to search for new physics beyond SM. Furthermore, the $t\bar{t}$ spin-correlation C can be measured at hadron colliders. As an application of our results, we further consider the contributions of the LHT model to $t\bar{t}$ spin correlation. We find that, with reasonable values of the free parameters, the relative ratio of LHT to SM for $t\bar{t}$ spin-correlation C can be over 100%.

ACKNOWLEDGMENTS

This work was supported in part by the National Natural Science Foundation of China under Grants No. 10675057 and 10875073, Specialized Research Fund for the Doctoral Program of Higher Education (SRFDP) (No. 200801650002), the Natural Science Foundation of the Liaoning Scientific Committee (No. 20082148), and Foundation of Liaoning Educational Committee (No. 2007T086).

APPENDIX

In this appendix, we give the form factors $A_c \sim H_c$ appearing in the vertex corrections. Here the vertex of the $St\bar{t}$ where S represents the scalar particle in LHT has the general form $i(g_V + g_A\gamma_5)$.

First we consider the irreducible triangle-loop correction, which is given in Fig. 7. Here q is the momentum of

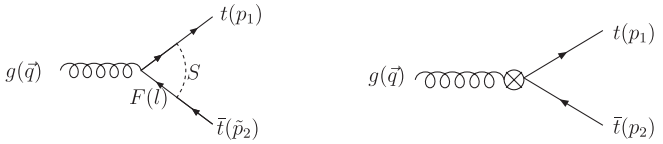

FIG. 7. Feynman diagram for the irreducible triangle-loop correction.

the gluon,t momentum is on shell while $\bar{t}$ momentum is off shell. Then the effective vertex can be written as follows:

$$\begin{aligned}\Gamma_\mu &= -ig_s T^a \mu^{2\epsilon} \int \frac{d^d l}{(2\pi)^d} i(g_V + g_A\gamma^5) \frac{i(\not{l} + \not{q} + m_F)}{(l+q)^2 - m_F^2} \\ &\quad \times \gamma_\mu \frac{i(\not{l} + m_F)}{(l)^2 - m_F^2} i(-g_V + g_A\gamma^5) \frac{1}{(l+q-p_1)^2 - m_S^2} \\ &= g_s T^a \mu^{2\epsilon} \int \frac{d^d l}{(2\pi)^d} \\ &\quad \times \frac{N_\mu}{[(l+q)^2 - m_F^2][(l)^2 - m_F^2][(l+q-p_1)^2 - m_S^2]} \end{aligned} \tag{A1}$$

with

$$\begin{aligned} N_\mu &= (g_V + g_A\gamma^5)(\not{l} + \not{q} + m_F)\gamma_\mu(\not{l} + m_F)(-g_V + g_A\gamma^5) \\ &= (g_V + g_A\gamma^5)(\not{l} + \not{q})\gamma_\mu \not{l}(g_V + g_A\gamma^5) \\ &\quad + m_F(g_V + g_A\gamma^5)\gamma_\mu \not{l}(-g_V + g_A\gamma^5) \\ &\quad + m_F(g_V + g_A\gamma^5)(\not{l} + \not{q})\gamma_\mu(-g_V + g_A\gamma^5) \\ &\quad + m_F^2(g_V + g_A\gamma^5)\gamma_\mu(g_V + g_A\gamma^5). \end{aligned} \tag{A2}$$

Then we can get:

$$\begin{aligned}\Gamma_\mu &= \frac{ig_s}{16\pi^2}[A\gamma_\mu + Bp_{1\mu}\not{q} Bp_{1\mu}\gamma_5 + Dp_{1\mu}\not{q}\gamma_5 + Ep_{1\mu} \\ &\quad + F\gamma_\mu\gamma_5 + G\not{q}\gamma_\mu + H\not{q}\gamma_\mu\gamma_5]. \end{aligned} \tag{A3}$$

The form factors for the other diagrams can be obtained in the same way. The factors in M_c and M_e are listed bellow.

1. Form factors appearing in M_c

$$\begin{aligned} A_c &= \frac{1}{16\pi^2}\frac{1}{4(p_1\cdot q)}\{(g_A^2 + g_V^2)[(B_0(0, m_F^2, m_F^2) \\ &\quad - B_0(p_1p_{2s}, m_F^2, m_S^2))(m_F^2 - m_S^2 + m_t^2)] \\ &\quad + 2(p_1\cdot q)(-1 + B_0(p_1p_{2s}, m_F^2, m_S^2) \\ &\quad - 4C_0(0, m_t^2, p_1p_{2s}, m_F^2, m_F^2, m_S^2)m_F^2)\} - \delta Z_V \end{aligned} \tag{A4}$$

$$\begin{aligned} B_c &= -\frac{1}{16\pi^2}\frac{1}{4[m_t^2 - 2(p_2\cdot q)](p_2\cdot q)^2}(g_A^2 + g_V^2)\{(B_0(0, m_F^2, m_F^2) - B_0(p_1p_{2s}, m_F^2, m_S^2))(m_F^2 - m_S^2 + m_t^2)m_t^2 \\ &\quad - 2[2B_0(p_1p_{2s}, m_F^2, m_S^2)m_F^2 - B_0(m_t^2, m_F^2, m_S^2)m_F^2 - 2B_0(p_1p_{2s}, m_F^2, m_S^2)m_S^2 + 2B_0(m_t^2, m_F^2, m_S^2)m_S^2 + m_t^2 \\ &\quad + B_0(p_1p_{2s}, m_F^2, m_S^2)m_t^2 - B_0(m_t^2, m_F^2, m_S^2)m_t^2 - 2C_0(0, m_t^2, p_1p_{2s}, m_F^2, m_F^2, m_S^2)m_F^2m_t^2 + A_0(m_F^2) + A_0(m_S^2)] \\ &\quad \times (p_1\cdot q) + 4(1 + 2C_0(0, m_t^2, p_1p_{2s}, m_F^2, m_F^2, m_S^2)m_F^2)(p_2\cdot q)^2\} \end{aligned} \tag{A5}$$

$$\begin{aligned} C_c &= \frac{1}{16\pi^2}\frac{1}{(p_1\cdot q)[m_t^2 - 2(p_1\cdot q)]m_t}[g_Ag_V(B_0(p_1p_{2s}, m_F^2, m_S^2) - B_0(m_t^2, m_F^2, m_S^2))m_t^2(m_F^2 - m_S^2 + m_t^2) \\ &\quad + 2(B_0(m_t^2, m_F^2, m_S^2)m_F^2 - B_0(m_t^2, m_F^2, m_S^2)m_S^2 - B_0(p_1p_{2s}, m_F^2, m_S^2)m_t^2 + B_0(m_t^2, m_F^2, m_S^2)m_t^2 \\ &\quad - A_0(m_F^2) + A_0(m_S^2)(p_1\cdot q))] \end{aligned} \tag{A6}$$

$$\begin{aligned} D_c &= \frac{1}{16\pi^2}\frac{-1}{2[m_t^2 - 2(p_2\cdot q)](p_2\cdot q)^2}g_Ag_V[(B_0(0, m_F^2, m_F^2) - B_0(p_1p_{2s}, m_F^2, m_S^2))m_t^2(m_F^2 - m_S^2 + m_t^2) \\ &\quad - 2(B_0(0, m_F^2, m_F^2)m_F^2 - 2B_0(p_1p_{2s}, m_F^2, m_S^2)m_F^2 - B_0(0, m_F^2, m_F^2)m_S^2 + 2B_0(p_1p_{2s}, m_F^2, m_S^2)m_S^2 - m_t^2 \\ &\quad + B_0(0, m_F^2, m_F^2)m_t^2 - B_0(p_1p_{2s}, m_F^2, m_S^2)m_t^2 - 2C_0(0, m_t^2, p_1p_{2s}, m_F^2, m_F^2, m_S^2)m_F^2m_t^2 + A_0(m_F^2) - A_0(m_S^2)](p_2\cdot q)^2 \end{aligned} \tag{A7}$$

$$\begin{aligned} E_c &= \frac{1}{16\pi^2}\frac{-1}{2(p_1\cdot q)}\{-2(B_0(p_1p_{2s}, m_F^2, m_S^2) - B_0(m_t^2, m_F^2, m_S^2))(g_A^2 - g_V^2)m_F + \frac{1}{m_t^3 - 2m_t(p_1\cdot q)} \\ &\quad \times [(g_A^2 + g_V^2)((B_0(p_1p_{2s}, m_F^2, m_S^2) - B_0(m_t^2, m_F^2, m_S^2))m_t^2(m_F^2 - m_S^2 + m_t^2) + 2(B_0(m_t^2, m_F^2, m_S^2)m_F^2 \\ &\quad - B_0(m_t^2, m_F^2, m_S^2)m_S^2 - B_0(p_1p_{2s}, m_F^2, m_S^2)m_t^2 - B_0(m_t^2, m_F^2, m_S^2)m_t^2 - A_0(m_F^2) + A_0(m_S^2))\cdot(p_1\cdot q)))]\} \end{aligned} \tag{A8}$$

$$\begin{aligned} F_c &= \frac{1}{16\pi^2}\frac{-1}{2(p_1\cdot q)}\{g_Ag_V[(B_0(p_1p_{2s}, m_F^2, m_S^2) - B_0(m_t^2, m_F^2, m_S^2))(m_F^2 - m_S^2 + m_t^2) + 2(-1 + B_0(p_1p_{2s}, m_F^2, m_S^2) \\ &\quad - 4C_0(0, m_t^2, p_1p_{2s}, m_F^2, m_F^2, m_S^2)m_F^2)(p_1\cdot q)]\} - \delta Z_A \end{aligned} \tag{A9}$$

$$G_c = \frac{1}{16\pi^2}\left\{C_0(0, m_t^2, p_1p_{2s}, m_F^2, m_F^2, m_S^2)(g_A^2 - g_V^2)m_F - \frac{(B_0(0, m_F^2, m_F^2) - B_0(p_1p_{2s}, m_F^2, m_S^2))(g_A^2 + g_V^2)m_t}{2(p_1 \cdot q)}\right\} \quad \text{(A10)}$$

$$H_c = \frac{1}{16\pi^2}\frac{1}{(p_1 \cdot q)}[g_A g_V(B_0(p_1p_{2s}, m_F^2, m_S^2) - B_0(m_t^2, m_F^2, m_S^2))m_t]. \quad \text{(A11)}$$

2. Form factors appearing in M_e

$$A_e = \frac{1}{16\pi^2}\frac{-1}{4(p_2 \cdot q)}\{(g_A^2 + g_V^2)[(B_0(m_t^2, m_S^2, m_F^2) - B_0(p_1p_{2s}, m_S^2, m_F^2))(m_F^2 - m_S^2 + m_t^2) + \frac{1}{(p_2 \cdot q)}(2 - 2B_0(p_1p_{2s}, m_S^2, m_F^2) + 4C_0(m_t^2, 0, p_1p_{2s}, m_S^2, m_F^2, m_F^2)(m_F^2 + m_S^2))]\} - \delta Z_V \quad \text{(A12)}$$

$$\begin{aligned} B_e = \frac{1}{16\pi^2}\frac{1}{4[m_t^2 - 2(p_2 \cdot q)](p_2 \cdot q)^2}\{&(g_A^2 + g_V^2)[(B_0(m_t^2, m_S^2, m_F^2) - B_0(p_1p_{2s}, m_S^2, m_F^2))(m_F^2 - m_S^2 + m_t^2)m_t^2 \\ &- 2(B_0(m_t^2, m_S^2, m_F^2)m_F^2 - B_0(p_1p_{2s}, m_S^2, m_F^2)m_F^2 - B_0^{12}m_S^2 - B_0(p_1p_{2s}, m_S^2, m_F^2)m_S^2 - m_t^2 + B_0(m_t^2, m_S^2, m_F^2)m_t^2 \\ &- B_0(p_1p_{2s}, m_S^2, m_F^2)m_t^2 - 2C_0(m_t^2, 0, p_1p_{2s}, m_S^2, m_F^2, m_F^2)m_F^2m_t^2 - A_0(m_F^2) - A_0(m_S^2))(p_2 \cdot q) \\ &- 4(1 + 2C_0(m_t^2, 0, p_1p_{2s}, m_S^2, m_F^2, m_F^2)m_F^2)(p_2 \cdot q)^2]\} \end{aligned} \quad \text{(A13)}$$

$$\begin{aligned} C_e = \frac{1}{16\pi^2}\frac{-1}{m_t[m_t^2 - 2(p_2 \cdot q)](p_2 \cdot q)}\{&g_A g_V[(B_0(m_t^2, m_S^2, m_F^2) - B_0(p_1p_{2s}, m_S^2, m_F^2))(m_F^2 - m_S^2 + m_t^2)m_t^2 \\ &- 2(B_0(m_t^2, m_S^2, m_F^2)m_F^2 - B_0(m_t^2, m_S^2, m_F^2)m_S^2 + B_0(m_t^2, m_S^2, m_F^2)m_t^2 - B_0(p_1p_{2s}, m_S^2, m_F^2)m_t^2 \\ &- A_0(m_F^2) + A_0(m_S^2))(p_2 \cdot q)]\} \end{aligned} \quad \text{(A14)}$$

$$\begin{aligned} D_e = \frac{1}{16\pi^2}\frac{-1}{2[m_t^2 - 2(p_2 \cdot q)](p_2 \cdot q)^2}\{&g_A g_V[(B_0(m_t^2, m_S^2, m_F^2) - B_0(p_1p_{2s}, m_S^2, m_F^2))(m_F^2 - m_S^2 + m_t^2)m_t^2 \\ &- 2(B_0(m_t^2, m_S^2, m_F^2)m_F^2 - B_0(p_1p_{2s}, m_S^2, m_F^2)m_F^2 + B_0(m_t^2, m_S^2, m_F^2)m_S^2 + B_0(p_1p_{2s}, m_S^2, m_F^2)m_S^2 - m_t^2 \\ &+ B_0(m_t^2, m_S^2, m_F^2)m_t^2 - B_0(p_1p_{2s}, m_S^2, m_F^2)m_t^2 - 2C_0(m_t^2, 0, p_1p_{2s}, m_S^2, m_F^2, m_F^2)m_F^2m_t^2 + A_0(m_F^2) - A_0(m_S^2))(p_2 \cdot q) \\ &- 4(1 + 2C_0(m_t^2, 0, p_1p_{2s}, m_S^2, m_F^2, m_F^2)m_F^2)(p_2 \cdot q)^2]\} \end{aligned} \quad \text{(A15)}$$

$$\begin{aligned} E_e = \frac{1}{16\pi^2}&2C_0(m_t^2, 0, p_1p_{2s}, m_S^2, m_F^2, m_F^2)(g_A^2(-m_F + m_t) + g_V^2(m_F + m_t)) + [(g_A^2(m_F - 2m_t) \\ &- g_V^2(m_F + 2m_t))(B_0(m_t^2, m_S^2, m_F^2) - B_0(p_1p_{2s}, m_S^2, m_F^2) - 2C_0(m_t^2, 0, p_1p_{2s}, m_S^2, m_F^2, m_F^2)(p_2 \cdot q))] \\ &+ \frac{1}{16\pi^2}\frac{1}{(p_2 \cdot q)}\left\{(g_A^2 + g_V^2)m_t[B_0(m_t^2, m_S^2, m_F^2) - B_0(p_1p_{2s}, m_S^2, m_F^2) \right. \\ &+ \frac{B_0(m_t^2, m_S^2, m_F^2)(-m_F^2 - m_S^2 + m_t^2) + A_0(m_F^2) + A_0(m_S^2)}{2m_t^2} + 2C_0(m_t^2, 0, p_1p_{2s}, m_S^2, m_F^2, m_F^2)(p_2 \cdot q) \\ &\left. + \frac{-A_0(m_F^2) + A_0(m_S^2) + B_0(p_1p_{2s}, m_S^2, m_F^2)(m_F^2 - m_S^2 - m_t^2 + 2(p_2 \cdot q))}{2[m_t^2 - 2(p_2 \cdot q)]}\right]\right\} \end{aligned} \quad \text{(A16)}$$

$$F_e = \frac{1}{16\pi^2}\frac{1}{2(p_2 \cdot q)}\{g_A g_V[(B_0(m_t^2, m_S^2, m_F^2) - B_0(p_1p_{2s}, m_S^2, m_F^2))(m_F^2 - m_S^2 + m_t^2) + (2 - 2B_0(p_1p_{2s}, m_S^2, m_F^2) + 4C_0(m_t^2, 0, p_1p_{2s}, m_S^2, m_F^2, m_F^2)(m_F^2 + m_S^2))\}(p_2 \cdot q)] - \delta Z_A \quad \text{(A17)}$$

$$G_e = \frac{1}{16\pi^2}\frac{1}{2(p_2\cdot q)} m_t (B_0(m_t^2, m_S^2, m_F^2) - B_0(p_1 p_{2s}, m_S^2, m_F^2))(g_A^2 + g_V^2) + 2C_0(m_t^2, 0, p_1 p_{2s}, m_S^2, m_F^2, m_F^2) \times m_F (p_2\cdot q)(g_A^2 - g_V^2) \quad \text{(A18)}$$

$$H_e = \frac{1}{16\pi^2}\frac{1}{(p_2\cdot q)^2} g_A g_V m_t [2(B_0(m_t^2, m_S^2, m_F^2) - B_0(p_1 p_{2s}, m_S^2, m_F^2))m_t^2 + (B_0(m_t^2, m_S^2, m_F^2) + B_0(p_1 p_{2s}, m_S^2, m_F^2) - 2B_0(0, m_F^2, m_F^2) + 2C_0(m_t^2, 0, p_1 p_{2s}, m_S^2, m_F^2, m_F^2)m_F^2 - 2C_0(m_t^2, 0, p_1 p_{2s}, m_S^2, m_F^2, m_F^2)m_S^2)(p_2\cdot q)], \quad \text{(A19)}$$

where A_0, B_0 and C_0 are the well-known one-point, two-point, and three-point scalar functions [44], which are given in terms of the Passarino-Veltman scalar functions. Here we use m_F (m_S) denote the mass of the fermion (scalar), q is the momentum of the gluon, $p_1 p_{2s} = m_t - 2(p_1\cdot q)$ is for $\bar{t}$ momentum off shell and $p_1 p_{2s} = m_t - 2(p_2\cdot q)$ is for t momentum is off shell.

3. Counter terms in Top-quark self-energy corrections

For the renormalization of the ultraviolet divergences appearing in the evaluation of the vertex and fermion self-energy corrections we use the counterterm method. The wave function renormalization constants can be determined from the top-quark self-energy diagrams, which can be decomposed in Fig. 8:

$$\Sigma(\not{p}) = \not{p}[\Sigma_V(p^2) + \Sigma_A(p^2)\gamma_5] + m_t\Sigma_S(p^2), \quad \text{(A20)}$$

Here:

$$\Sigma_V = -(g_A^2 + g_V^2)B_1 \quad \text{(A21)}$$

$$\Sigma_A = 2g_A g_V B_1 \quad \text{(A22)}$$

$$\Sigma_S = \frac{m_F}{m_t}(g_V^2 - g_A^2)B_0 \quad \text{(A23)}$$

With:

$$B_1 = \frac{1}{2p^2}[A_0(m_F^2) - A_0(m_S^2) - (m_F^2 - m_S^2 + p^2)B_0] \quad \text{(A24)}$$

$$B_0 = B_0(p^2, m_F^2, m_S^2). \quad \text{(A25)}$$

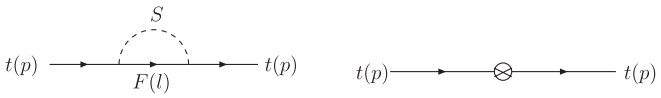

FIG. 8. Feynman diagram for top-quark self-energy correction.

In the on-shell scheme, the finite parts of the counter terms are determined by the requirement that the residue of the fermion propagator is equal to one, which fixes the wave function renormalization constraints by

$$\delta Z_V = -\Sigma_V(p^2 = m_t^2) - 2m_t^2\frac{\partial}{\partial p^2}(\Sigma_V + \Sigma_S)\mid_{p^2=m_t^2} \quad \text{(A26)}$$

$$\delta Z_A = -\Sigma_A(p^2 = m_t^2) \quad \text{(A27)}$$

$$\delta m_t = \Sigma_S(m_t^2) - 2m_t^2\frac{\partial}{\partial p^2}(\Sigma_V + \Sigma_S)\mid_{p^2=m_t^2} \quad \text{(A28)}$$

In the LHT model, they are given by

$$\delta Z_A = \frac{1}{16\pi^2}\frac{g_A g_V}{m_t^2}[A_0(m_S^2) - A_0(m_F^2) + (m_F^2 - (m_S^2) + m_t^2)B_0] \quad \text{(A29)}$$

$$\delta Z_V = \frac{1}{16\pi^2}\frac{g_A^2 + g_V^2}{2m_t^2}[A_0(m_S^2) - A_0(m_F^2) + (m_F^2 - m_S^2 + m_t^2)]B_0(m_t^2) + \frac{1}{16\pi^2}[(g_A^2 + g_A^2)(-m_F^2 + m_S^2 - m_t^2) - (g_A^2 - g_A^2)2m_t m_F]B_0'(m_t^2); \quad \text{(A30)}$$

$$\delta m_t = -\frac{1}{16\pi^2}[2(g_A^2 + g_V^2)m_t m_F + (g_A^2 + g_V^2) \times (m_F^2 - m_S^2 + m_t^2)]B_0'(m_t^2) + \frac{1}{16\pi^2}\frac{1}{m_t^2} \times \{(g_A^2 + g_V^2)[A_0(m_S^2) - A_0(m_F^2)] + [(g_A^2 + g_V^2)(m_F^2 - m_S^2) + (g_A^2 - g_V^2)m_t m_F] \times B_0(m_t^2)\}; \quad \text{(A31)}$$

with

$$B_0(m_t^2) \equiv B_0(m_t^2; m_S^2, m_F^2), \quad B_0'(m_t^2) \equiv \frac{\partial}{\partial P^2}B_0(m_t^2; m_S^2, m_F^2)\mid_{p^2=m_t^2}. \quad \text{(A32)}$$

[1] F. Abe *et al.* (CDF Collaboration), Phys. Rev. Lett. **74**, 2626 (1995).

[2] S. Abachi *et al.* (D0 Collaboration), Phys. Rev. Lett. **74**, 2632 (1995).

[3] C. T. Hill and E. H. Simmons, Phys. Rep. **381**, 235 (2003).

[4] I. Bigi and H. Krasemann, Z. Phys. C **9**, 197 (1981); I. Bigi *et al.*, Phys. Lett. B **181**, 157 (1986); M. Jezabek and J. H. Kühn, Nucl. Phys. **B320**, 20 (1989); A. Czarnecki, M. Jezabek, and J. H. Kühn, Nucl. Phys. **B351**, 70 (1991); A. Brandenburg, Z. G. SI, and P. Uwer, Phys. Lett. B **539**, 235 (2002).

[5] W. Beenakker, W. L. van Neerven, R. Meng, G. A. Schuler, and J. Smith, Nucl. Phys. **B351**, 507 (1991).

[6] J. A. Aguilar-saavedra *et al.* (ECFA/DESY LC Physics Working Group).

[7] S. Heinemeyer, W. Hollik, A. M. Weber, and G. Weiglein, arXiv:0711.0456; J. Erler and P. Langacker, Acta Phys. Pol. B **39**, 2595 (2008).

[8] A. Ghosal, Y. Koide, and H. Fusaoka, Phys. Rev. D **64**, 053012 (2001); P. M. Ferreira, R. B. Guedes, and R. Santos, Phys. Rev. D **75**, 055015 (2007); E. O. Iltan, Eur. Phys. J. C **56**, 113 (2008); R. Benbrik and C.-K. Chua, Phys. Rev. D **78**, 075025 (2008).

[9] J. H. Kühn, Nucl. Phys. **B237**, 77 (1984).

[10] V. D. Barger, J. Ohnemus, and R. J. Phillips, Int. J. Mod. Phys. A **4**, 617 (1989).

[11] T. Arens and L. M. Sehgal, Nucl. Phys. **B393**, 46 (1993); Phys. Lett. B **302**, 501 (1993).

[12] G. Mahlon and S. Parke, Phys. Rev. D **53**, 4886 (1996).

[13] T. Stelzer and S. Willenbrock, Phys. Lett. B **374**, 169 (1996).

[14] D. Chang, S. C. Lee, and A. Soumarokov, Phys. Rev. Lett. **77**, 1218 (1996); A. Brandenburg, Phys. Lett. B **388**, 626 (1996); G. Mahlon and S. Parke, Phys. Lett. B **411**, 173 (1997).

[15] W. Bernreuther, A. Brandenburg, Z. G. Si, and P. Uwer, Phys. Lett. B **509**, 53 (2001); Phys. Rev. Lett. **87**, 242002 (2001); Nucl. Phys. **B690**, 81 (2004); W. Bernreuther, M. Fucker, and Z. G. Si, Phys. Rev. D **74**, 113005 (2006); **78**, 017503 (2008); Phys. Lett. B **633**, 54 (2006).

[16] D. Atwood, A. Aeppli, and A. Soni, Phys. Rev. Lett. **69**, 2754 (1992).

[17] G. L. Kane, G. A. Ladinsky, and C. P. Yuan, Phys. Rev. D **45**, 124 (1992).

[18] C. R. Schmidt and M. E. Peskin, Phys. Rev. Lett. **69**, 410 (1992).

[19] A. Brandenburg and J. P. Ma, Phys. Lett. B **298**, 211 (1993); W. Bernreuther and A. Brandenburg, Phys. Lett. B **314**, 104 (1993); Phys. Rev. D **49**, 4481 (1994).

[20] P. Haberl, O. Nachtmann, and A. Wilch, Phys. Rev. D **53**, 4875 (1996); K. Cheung, Phys. Rev. D **55**, 4430 (1997).

[21] B. Grzadkowski, B. Lampe, and K. J. Abraham, Phys. Lett. B **415**, 193 (1997).

[22] W. Bernreuther, M. Flesch, and P. Haberl, Phys. Rev. D **58**, 114031 (1998); W. Bernreuther, A. Brandenburg, and M. Flesch, arXiv:hep-ph/9812387.

[23] D. Atwood, S. Bar-Shalom, G. Eilam, and A. Soni, Phys. Rev. D **69**, 033006 (2004); W. Khater and P. Osland, Nucl. Phys. **B661**, 209 (2003).

[24] K. Y. Lee, H. S. Song, J. H. Song, and C. Yu, Phys. Rev. D **60**, 093002 (1999); K. Y. Lee, S. C. Park, H. S. Song, and C. Yu, Phys. Rev. D **63**, 094010 (2001).

[25] K. Y. Lee, S. C. Park, H. S. Song, J. H. Song, and C. Yu, Phys. Rev. D **61**, 074005 (2000); I. Sahin, Eur. Phys. J. C **60**, 431 (2009); Masato Arai, Nobuchika Okada, Karel Smolek, and Vladislav Simak, Acta Phys. Pol. B **40**, 93 (2009); B. Sahin, arXiv:0802.1937.

[26] C. X. Yue, L. N. Wang, J. Phys. G **34**, 139 (2007).

[27] H.-Y. Zhou and C.-S. Li, Phys. Rev. D **55**, 4421 (1997); W. Hollik, W. M. Mosle, C. Kao, and D. Wa keroth, arXiv: hep-ph/9711419; H.-Y. Zhou and C.-S. Li, Commun. Theor. Phys. **30**, 465 (1998); S. Berge, W. Hollik, W. M. Mosle, and D. Wa ckeroth, Phys. Rev. D **76**, 034016 (2007); D. A. Ross and M. Wiebusch, J. High Energy Phys. 11 (2007) 041.

[28] C.-S. Li, B.-Q. Hu, J.-M. Yang, and C.-G. Hu, Phys. Rev. D **52**, 5014 (1995); J. M. Yang and C. S. Li, Phys. Rev. D **54**, 4380 (1996); J. Kim, J. L. Lopez, D. V. Nanopoulos, and R. Rangarajan, Phys. Rev. D **54**, 4364 (1996).

[29] C.-S. Li, H.-Y. Zhou, Y.-L. Zhu, and J.-M. Yang, Phys. Lett. B **379**, 135 (1996); S. Alam, K. Hagiwara, and S. Matsumoto, Phys. Rev. D **55**, 1307 (1997); Z. Sullivan, Phys. Rev. D **56**, 451 (1997); C.-S. Li, R. J. Oakes, J. M. Yang, and C. P. Yuan, Phys. Lett. B **398**, 298 (1997).

[30] A. Stange and S. Willenbrock, Phys. Rev. D **48**, 2054 (1993); H.-Y. Zhou, C.-S. Li, and Y.-P. Kuang, Phys. Rev. D **55**, 4412 (1997); W. Hollik, W. M. Mosle, and D. Wa keroth, Nucl. Phys. **B516**, 29 (1998); C. Kao and D. Wackeroth, Phys. Rev. D **61**, 055009 (2000).

[31] H.-C. Cheng and I. Low, J. High Energy Phys. 09 (2003) 051.

[32] H.-C. Cheng and I. Low, J. High Energy Phys. 08 (2004) 061.

[33] I. Low, J. High Energy Phys. 10 (2004) 067; J. Hubisz and P. Meade, Phys. Rev. D **71**, 035016 (2005); C. S. Chen, Kingman Cheung, and T.-C. Yuan, Phys. Lett. B **644**, 158 (2007); C.-R. Chen, K. Tobe, and C.-P. Yuan, Phys. Lett. B **640**, 263 (2006).

[34] J. Hubisz, P. Meade, A. Noble, and M. Perelstein, J. High Energy Phys. 01 (2006) 135.

[35] J. M. Cornwall, D. N. Levin, and G. Tiktopoulos, Phys. Rev. D **10**, 1145 (1974); C. E. Vayonakis, Nuovo Cimento Soc. Ital. Fis. A **17**, 383 (1976); B. W. Lee, C. Quigg, and H. B. Thacker, Phys. Rev. D **16**, 1519 (1977).

[36] M. S. Chanowitz and M. K. Gaillard, Nucl. Phys. **B261**, 379 (1985); G. J. Gounaris, R. Kogerler, and H. Neufeld, Phys. Rev. D **34**, 3257 (1986); Y.-P. Yao and C. P. Yuan, Phys. Rev. D **38**, 2237 (1988).

[37] J. Bagger and C. Schmidt, Phys. Rev. D **41**, 264 (1990); H. G. J. Veltman, Phys. Rev. D **41**, 2294 (1990); H.-J. He, Y.-P. Kuang, and X.-Y. Li, Phys. Rev. Lett. **69**, 2619 (1992); R. Barbierib, M. Beccariab, P. Ciafalonib, G. Curcia, and A. Viceréb, Nucl. Phys. **B409**, 105 (1993).

[38] H.-J. He, Y.-P. Kuang, and X.-Y. Li, Phys. Rev. D **49**, 4842 (1994); Phys. Lett. B **329**, 278 (1994); H.-J. He, Y.-P. Kuang, and C. P. Yuan, Phys. Rev. D **51**, 6463 (1995).

[39] A. Dobado and J. R. Pelaez, Nucl. Phys. **B425**, 110 (1994); Phys. Lett. B **329**, 469 (1994); R. Barbierib, M. Beccariab, P. Ciafalonib, G. Curcia, and A. Viceréb, Phys. Lett. B **288**, 95 (1992).

[40] Monika Blanke, Andrzej J. Buras, Anton Poschenrieder *et al.*, J. High Energy Phys. 05 (2007) 013.

[41] Qing-Hong Cao, Chuan-Ren Chen, F. Larios, and C.-P. Yuan, Phys. Rev. D **79**, 015004 (2009).
[42] J. Pumplin *et al.* (CTEQ Collaboration), J. High Energy Phys. 02 (2006) 032.
[43] P. Dey, S. K. Gupta, and B. Mukhopadhyaya, Phys. Lett. B **674**, 188 (2009).
[44] G. Passarino and M. J. G. Veltman, Nucl. Phys. **B160**, 151 (1979).